Additive Manufacturing Letters 1 (2021) 100014

Contents lists available at ScienceDirect

Additive Manufacturing Letters

journal homepage: www.elsevier.com/locate/addlet

A convolution-based approach to cold spray additive manufacturing

F. Venturi [a], N. Gilfillan [b], T. Hussain [a,*]

[a] Faculty of Engineering, University of Nottingham, University Park, Nottingham NG7 2RD, United Kingdom
[b] Dycomet UK Ltd., Newton, Hyde, Cheshire SK14 4EU, United Kingdom

ARTICLE INFO

Keywords:
CSAM
Low pressure cold spray
Convolution
Digitalisation
Predictive manufacturing

ABSTRACT

Cold Spray Additive Manufacturing (CSAM) is a well-established technology that has recently attracted interest for forming 3D shapes in a fast and scalable fashion. Nonetheless, the resulting surface of cold sprayed parts normally requires post-deposition machining to achieve the desired surface finish. In this work, a convolution-based digital framework for CSAM yield and surface finish prediction able to calculate the optimal interline distance to reduce surface waviness was developed. The aim is to minimise post-deposition treatments, thereby reducing production time, material waste and costs. This method is applicable beyond CSAM and can be of interest for other additive manufacturing techniques.

1. Introduction

Cold Spray Additive Manufacturing (CSAM), is a well-established materials deposition technology that has proved suitable for coating, repair and additive manufacturing [1]. In CSAM, powder particles of 5–45 μm size are transported by a stream of supersonic accelerating gas through a converging-diverging de Laval nozzle and deposited onto a substrate upon high-velocity impact. The momentum of the particles at impact yields a high strain rate plastic deformation of both the particle and the substrate [2], yielding to interlock or cold welding by adiabatic shear instability [3], and ultimately achieving bonding [4]. The feedstock particles are deposited when their velocity at impact is within a range called deposition window [5]; outside this range, deposition efficiency approaches zero, until no deposition or erosion take place [6]. An intrinsic characteristic of the CSAM process is the distribution of velocities the particles acquire when sprayed. Considering particles of equal size and shape, due to boundary effects of the nozzle walls on the gas flow, particles at the centre of the nozzle will be accelerated more than those closer to the boundaries [7], yielding a radial distribution of deposition efficiency which gives the characteristic conical shape of the deposition. As a result, when building up an extended deposition over a wide area, an uneven deposition thickness and typical crater-like shapes are formed as a by-product of this characteristic deposition shape. Consequently, additional crater-filling deposition and material removal are required to obtain a smooth surface finish of the desired thickness [8], increasing materials waste, costs and manufacturing time. A possible mitigation to this problem can be offered by convolution [9], for which by knowing the shape or fingerprint of the deposition process, it is possible to predict the final deposition shape for a given additive manufacturing pattern. Recent approaches either theoretical [10], machine learning-based [11,12], differential equation-based [13] and based on gaussian approximation coupled with ABB RobotStudio simulation [14] have been proposed. These methods share a Gaussian approach to spray profile fitting and tackle the prediction task with various mathematical frameworks, yielding algorithm of different computational cost. However, a convolutional approach to CSAM, which would be an easier and computationally cheap solution, is still missing and can be an additional powerful tool. In this work, a method is presented to pre-assess the deposition yield and shape, and to select the optimal deposition parameters to obtain a desired surface finish in order to minimise the need for post-deposition surface treatments.

2. Material and methods

The CSAM samples in this work were deposited by Dymet DY423 (Dycomet, United Kingdom) on Al6082-T6 substrates. The feedstock used were the commercial powder blends K-10–01 (nominal composition Al_2O_3 60–70 wt.%, Al 30–40 wt.%) and K-20-11 (Zn 38–42 wt.%, Al_2O_3 23–27 wt.%, Al 33–37 wt.%) supplied by Dycomet. These will hereafter be referred to as C-Al and C-AlZn, respectively, where C stands for ceramic. The spray parameters used were a feed rate of 0.6 g/s, 5.6 bar air pressure and 10 mm stand-off distance. Optimal heating values were chosen for each powder: Dymet setting T4 for C-Al (equivalent to ~500 °C air temperature) and T3 for C-AlZn (~400 °C). A stainless steel nozzle was used, 120 mm long and with 5 mm internal diameter.

Three types of samples were obtained from the two powders: spot, line and step. In spot deposition the nozzle was directed at a fixed point for a dwell time of 1, 2, 3, 4 and 5 s, in line deposition the nozzle was

* Corresponding author.
E-mail address: tanvir.hussain@nottingham.ac.uk (T. Hussain).

https://doi.org/10.1016/j.addlet.2021.100014
Received 13 September 2021; Received in revised form 19 October 2021; Accepted 19 October 2021

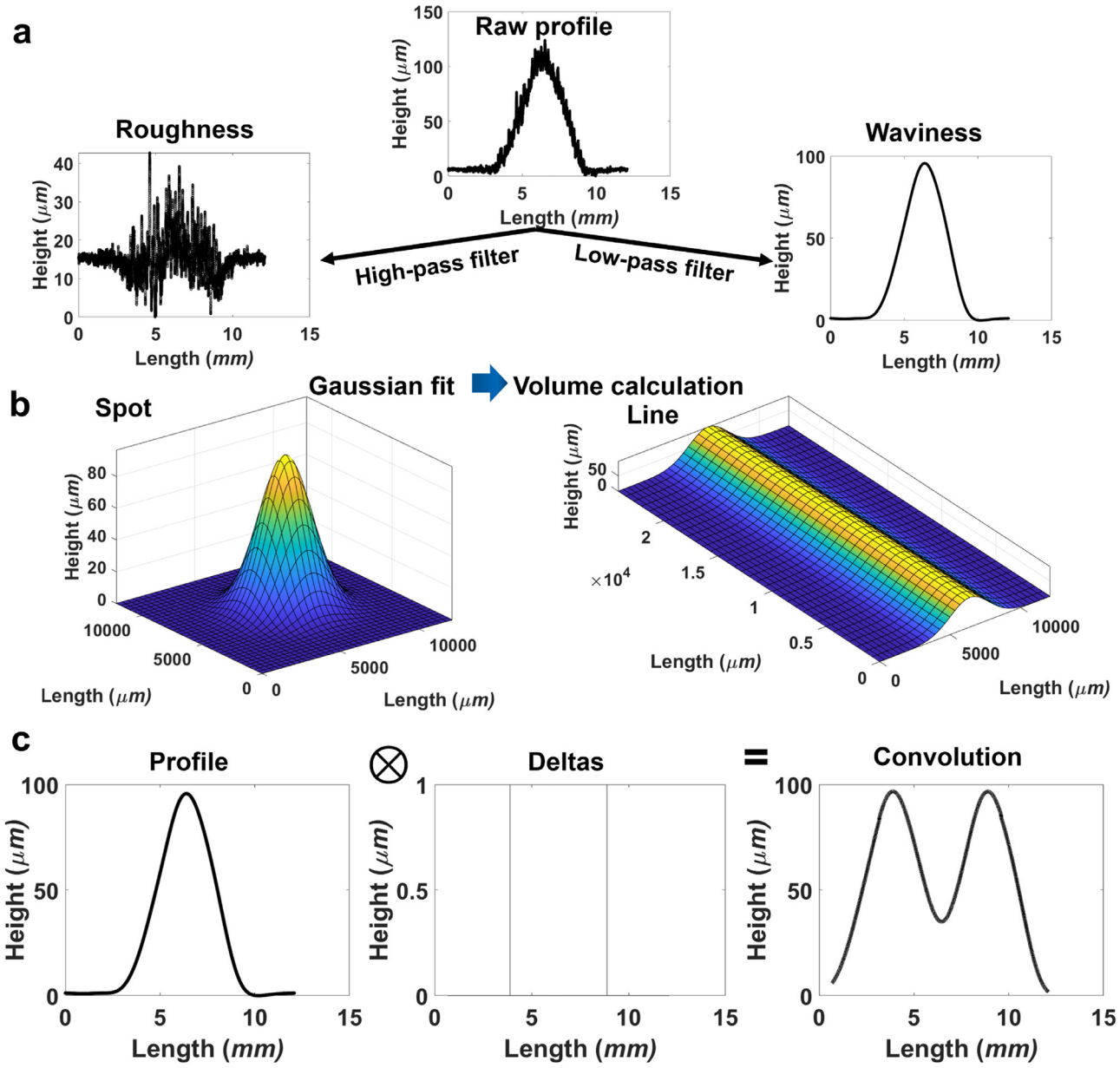

Fig. 1. CSAM digital framework method – (a) Measured profile filtering. (b) Gaussian fit for spot and line volume and spray yield calculation. (c) Prediction of the final surface waviness by convolution.

moving in a fixed direction at a 5, 10, 20, 50 and 100 mm/s traverse speed, whereas in step two lines were performed at an interline distance, or step, of 1, 2, 3, 4 and 5 mm (at 5 mm/s). The surface profiles of the samples were measured along a single line across the depositions using a Talysurf contact profilometer (Taylor Hobson, United Kingdom); an Alicona InfiniteFocus G5+ (Bruker, Austria) was used for two samples which exceeded the Talysurf measurement range. The spatial resolution was 0.5 µm along x and 0.8 nm along z for the Talysurf and 0.44 µm along x and y and 10 nm along z for the Alicona. The profiles were analysed with the software Mountains Map and Matlab using a 1.5 mm Gaussian cut-off length.

The measured profiles were analysed according to the process shown in Fig. 1. The measured raw profiles were levelled, and gaussian high- and low-pass filters were applied to decouple the roughness from the waviness information, as in Fig. 1a. In this work, the waviness information was used, as it is the one giving the overall information on the deposition shape. The roughness information was disregarded as it cannot be predicted or optimised by the proposed method. As shown in Fig. 1b, for the spot depositions, the 3D Gaussian fit allowed to calculate the deposited volume of material. For the line depositions, the waviness profile was used to generate a 3D line deposition used to calculate the deposited material volume. The deposition yield was calculated as $Y = \frac{V}{t}$ where V is the deposited volume and t the deposition time. Finally, as shown in Fig. 1c, the superposition shape of two subsequent line depositions was simulated by convoluting the line profiles with two delta distributions using the Matlab *conv* function, at a given distance of 1, 2, 3, 4 and 5 mm to compare with the experimental results.

3. Results and discussion

3.1. Deposition yield

The deposition yield was studied for spot and line deposition, as presented in Fig. 2. In the spot case (Fig. 2a) the deposition yield at 1 s is higher for C-Al than for C-AlZn, then at 2 s and 3 s it decreases for C-Al and increases for C-AlZn, reaching a steady value at 4 s and

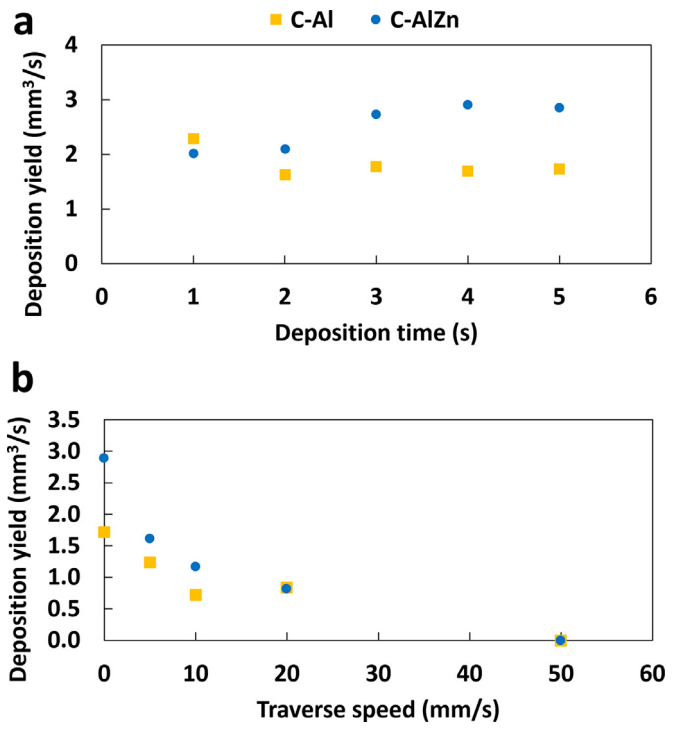

Fig. 2. Deposition yield measured for spot (a) and line (b) depositions, showing steady deposition yield after 3 s and decrease of deposition yield with increasing traverse speed, approaching zero at 50 mm/s. The variability is below 5%.

5 s with average values of yield $Y_{C\text{-}Al}$ = (1.72 ± 0.02) mm^3/s and $Y_{C\text{-}AlZn}$ = (2.88 ± 0.02) mm^3/s. The inversion in deposition yield between C-Al and C-AlZn shows that the former gives better yield when sprayed onto the bare substrate, whereas the second when sprayed on itself. In the line case (Fig. 2b), the deposition yield decreases for increasing traverse speed, reaching no measurable deposition at 50 mm/s. At this point, a threshold traverse speed has been overtaken. The material stops building upon itself and only forms single-particle bonding with the substrate – a typical configuration for single-particle impact analysis – therefore, only a layer of scattered particles and some erosion are present. The 20 mm/s velocity interestingly shows an increase of the C-Al deposition yield, confirming its tendency to have higher deposition efficiency on the bare substrate. The explanation of this lies in the presence of twice as much ceramic (Al_2O_3) in C-Al compared to C-AlZn. The ceramic acts as a shot-peening agent: it favours the metal deposition and at the same time it compacts the existing deposition, but consequently not all the ceramic particles are able to get deposited, and part of them is bounced away, not contributing to the deposition.

3.2. Surface profile prediction by convolution

The cross-sectional profiles from the line depositions were used to predict the surface profile given by a superposition of those at a given interline distance. In Fig. 3, simulated and experimental superposition of line deposition at 1–5 mm distance is presented for powders C-Al (a) and C-AlZn (b). Here, the superposition of parallel lines is considered. The beginning, the end and the turns of the spray path in a raster configuration are not studied as they normally occur outside the sample area in a typical cold spray configuration; however, the convolution method can be used with more complex path geometries. If the two lines are too close, the deposition occurs on top of itself, keeping the Gaussian-like shape and increasing in height compared to the single line. If, on the other hand, the two lines are too far apart, the deposition takes the shape of two partially overlapped Gaussian distributions, with a trough in between. Neither of these two cases is optimal for CSAM deposition, as the first case results in an excessive deposition, and the second results in excessive surface waviness. In both cases, machining will eventually be required for a smooth surface finish. The aimed outcome would be characterised by a flat top, with no trough between the two profiles, which occurs around 3–4 mm as visible both in Fig. 3a and b.

It should be noticed that this method is effective in predicting the shape, but not as much in predicting the yield, as the discrepancy in height between simulation and experiment both in Fig. 3a and b reveals. This is due to the different yield when spraying on the flat substrate or on a previously deposited, tilted line deposition. However, the discrepancy in height is the lowest (around 10%) at the values of interest, 3 and 4 mm step. This method would be applicable also for predicting the shape of multiple additional lines without affecting the previous results.

3.3. Optimal interline distance calculation

The optimal distance between two neighbouring lines was calculated by an algorithm based on a loop that calculates iteratively the two lines getting closer and stops at the first distance for which the trough between them disappears i.e. when the profile curve first has a single maximum. This yielded optimal line distances *d* for the two materials of $d_{C\text{-}Al}$ = 3.77 mm and $d_{C\text{-}AlZn}$ = 3.06 mm. These values are the outcome of the algorithm: experimentally, taking into account the experimental uncertainties of the input measurements, a range of ± 0.01 mm would be an acceptable interline distance for practical applications. The surface finish is as flat as the initial line profiles allow and can be used as an optimised interline distance for an extended CSAM deposition, reducing the final surface waviness and avoiding excessive deposition thickness. Note that these values are valid only for these materials at the spray conditions chosen: the acquisition of a new reference profile will be needed for every change in the process, be it intrinsic (material, pressure, traverse speed, temperature, substrate, stand-off distance) or extrinsic (powder flowability, humidity, heating efficiency, nozzle wear). In fact, it should be noted that the proposed method does not take into account parameters such as the powder particle size distribution, the powder distribution in the flow or the deposition efficiency. Therefore, the method has the above limitation of requiring a new profile acquisition for any new set of intrinsic and extrinsic parameters, but has the benefit of being applicable to any of these combinations, regardless of the individual experimental details. The convolution approach was chosen as it can handle any 2D track path geometry and would therefore be easier to generalise to complex shape deposition, 3D deposition, and deconvolution to calculate optimal track for 3D shapes.

4. Conclusion

A digitalised method for CSAM was developed, providing deposition yield, predicting surface finish by convolution and informing about the optimal interline distance to minimise surface waviness and excessive deposition thickness. The convolution method offers a semi-quantitative approach to deposition shape prediction; a quantitative approach would need to take into account the variation of deposition efficiency due to substrate material, shape and roughness. To implement this strategy in a spray run, an initial single line should be sprayed at the target traverse velocity and the cross-sectional profile should be measured. The algorithm will inform the operator as for which interline distance to set to reduce spray time, post-deposition machining time and material wastage.

Declaration of Competing Interest

The authors declare that they have no known competing financial interests or personal relationships that could have appeared to influence the work reported in this paper.

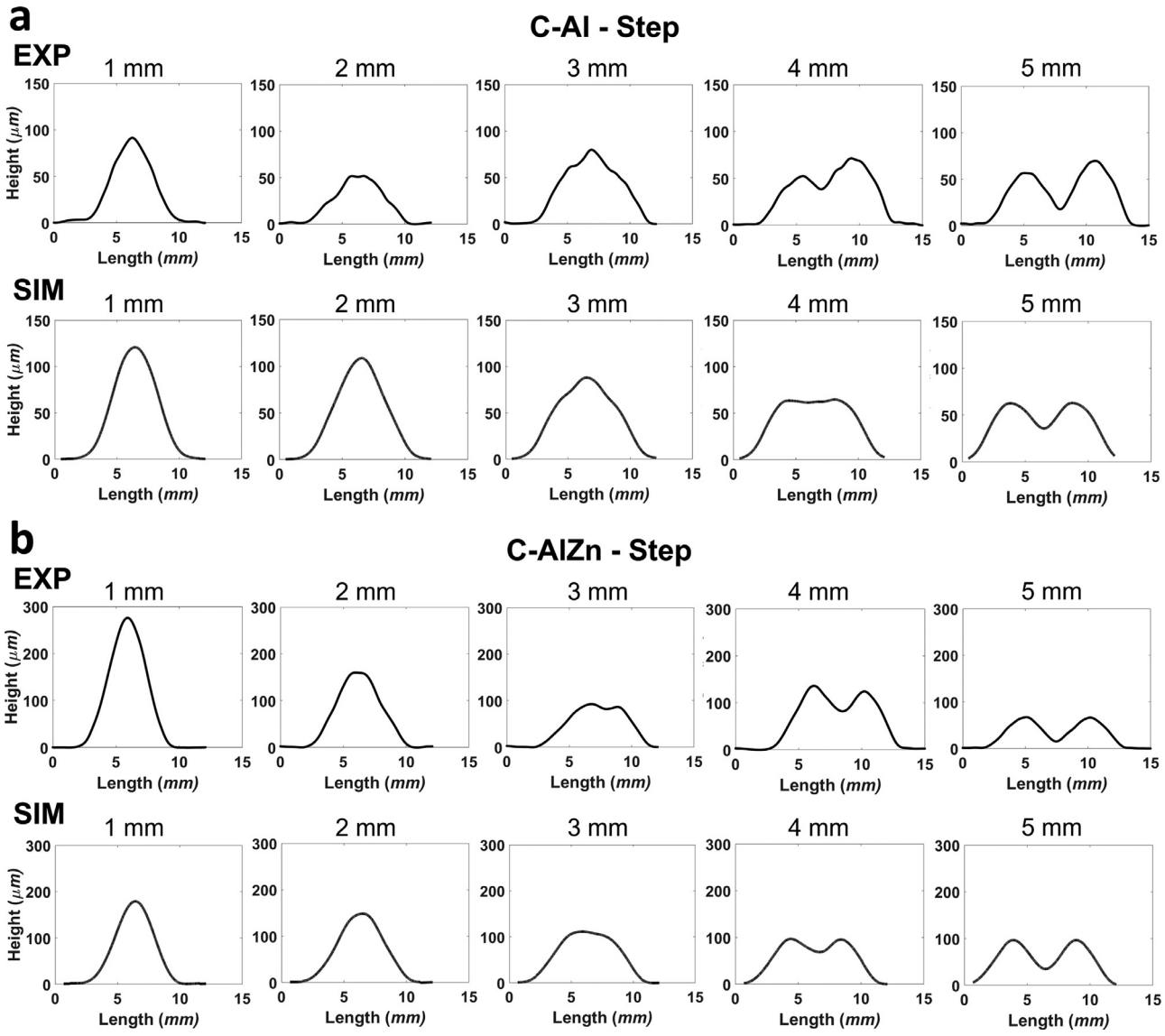

Fig. 3. Experimental and simulated cross-sectional profile for step depositions at 1–5 mm interline distance for (a) C-Al and (b) C-AlZn powders. Profile heights have been made uniform for allowing better shape comparison; the different height can be noted in the y axes.

Acknowledgements

This work was supported by the Engineering and Physical Sciences Research Council Network Plus in Digitalised Surface Manufacturing [grant number EP/S036180/1]. This work has been conducted in the framework of Innovate UK project "Digitalization infrastructure and expert system for cold spray additive manufacturing (DigiCSAM)" [Project No. 105624] led by Dycomet UK Ltd. The authors acknowledge Jake Gilfillan at Dycomet, the Manufacturing Metrology Team at the University of Nottingham for access to the profilometry facilities, Dr Luc Pouliot for useful discussions, suggestions and careful proofreading, and Dr Vincenzo Grillo for initial discussions on the topic.

References

[1] R.N. Raoelison, Y. Xie, T. Sapanathan, M.P. Planche, R. Kromer, S. Costil, et al., Cold gas dynamic spray technology: a comprehensive review of processing conditions for various technological developments till to date, Addit. Manuf. 19 (2018) 134–159, doi:10.1016/j.addma.2017.07.001.

[2] X. Wang, F. Feng, M.A. Klecka, M.D. Mordasky, J.K. Garofano, T. El-Wardany, et al., Characterization and modeling of the bonding process in cold spray additive manufacturing, Addit. Manuf. 8 (2015) 149–162, doi:10.1016/j.addma.2015.03.006.

[3] M. Grujicic, C.L. Zhao, W.S. De Rosset, D. Helfritch, Adiabatic shear instability based mechanism for particles/substrate bonding in the cold-gas dynamic-spray process, Mater. Des. 25 (2004) 681–688, doi:10.1016/j.matdes.2004.03.008.

[4] T. Schmidt, H. Assadi, F. Gärtner, H. Richter, T. Stoltenhoff, H. Kreye, et al., From particle acceleration to impact and bonding in cold spraying, J. Therm. Spray Tech. 18 (2009) 794, doi:10.1007/s11666-009-9357-7.

[5] T. Schmidt, F. Gärtner, H. Assadi, H. Kreye, Development of a generalized parameter window for cold spray deposition, Acta Mater. 54 (2006) 729–742, doi:10.1016/j.actamat.2005.10.005.

[6] S.V. Klinkov, V.F. Kosarev, Measurements of cold spray deposition efficiency, J. Therm. Spray Tech. 15 (2006) 364–371, doi:10.1361/105996306X124365.

[7] D.L. Gilmore, R.C. Dykhuizen, R.A. Neiser, M.F. Smith, T.J. Roemer, Particle velocity and deposition efficiency in the cold spray process, J. Therm. Spray Tech. 8 (1999) 576–582, doi:10.1361/105996399770350278.

[8] S. Yin, P. Cavaliere, B. Aldwell, R. Jenkins, H. Liao, W. Lid, et al., Cold spray additive manufacturing and repair: fundamentals and applications, Addit. Manuf. 21 (2018) 628–650, doi:10.1016/j.addma.2018.04.017.

[9] R. Tolimieri, M. An, C Lu, Algorithms for Discrete Fourier Transform and Convolution, Springer, New York, 1989.

[10] Q. Huang, Y. Wang, M. Lyu, W. Lin, Shape deviation generator—a convolution framework for learning and predicting 3-D printing shape accuracy, IEEE Trans. Autom. Sci. Eng. 17 (2020) 1486–1500, doi:10.1109/TASE.2019.2959211.

[11] I.M. Nault, G.D. Ferguson, A.T. Nardi, Multi-axis tool path optimization and deposition modeling for cold spray additive manufacturing, Addit. Manuf. 38 (2021) 101779, doi:10.1016/j.addma.2020.101779.

[12] D. Ikeuchi, A. Vargas-Uscategui, X. Wu, P.C. King, Neural network modelling of track profile in cold spray additive manufacturing, Materials 12 (2019) 2827, doi:10.3390/ma12172827.
[13] D. Vanerio, J. Kondas, M. Guagliano, S. Bagherifard, 3D modelling of the deposit profile in cold spray additive manufacturing, J. Manuf. Processes 67 (2021) 521–534, doi:10.1016/j.jmapro.2021.05.013.
[14] H. Wu, X. Xie, M. Liu, C. Verdy, Y. Zhang, H. Liao, S. Deng, Stable layer-building strategy to enhance cold-spray-based additive manufacturing, Addit. Manuf. 35 (2020) 101356, doi:10.1016/j.addma.2020.101356.